A simplified description of the evolution of organic aerosol composition in the atmosphere

C. L. Heald,[1] J. H. Kroll,[2] J. L. Jimenez,[3] K. S. Docherty,[3] P. F. DeCarlo,[4,5] A. C. Aiken,[3,6] Q. Chen,[7] S. T. Martin,[7] D. K. Farmer,[3] and P. Artaxo[8]

[1] Organic aerosol (OA) in the atmosphere consists of a multitude of organic species which are either directly emitted or the products of a variety of chemical reactions. This complexity challenges our ability to explicitly characterize the chemical composition of these particles. We find that the bulk composition of OA from a variety of environments (laboratory and field) occupies a narrow range in the space of a Van Krevelen diagram (H:C versus O:C), characterized by a slope of ∼−1. The data show that atmospheric aging, involving processes such as volatilization, oxidation, mixing of air masses or condensation of further products, is consistent with movement along this line, producing a more oxidized aerosol. This finding has implications for our understanding of the evolution of atmospheric OA and representation of these processes in models. **Citation:** Heald, C. L., J. H. Kroll, J. L. Jimenez, K. S. Docherty, P. F. DeCarlo, A. C. Aiken, Q. Chen, S. T. Martin, D. K. Farmer, and P. Artaxo (2010), A simplified description of the evolution of organic aerosol composition in the atmosphere, *Geophys. Res. Lett.*, *37*, L08803, doi:10.1029/2010GL042737.

1. Introduction

[2] Organic aerosol (OA) makes up an important, sometimes dominant, fraction of submicron particulate matter in the atmosphere [*Zhang et al.*, 2007]. However, models are generally unsuccessful in reproducing the observed magnitudes and variability of these particles [*Capes et al.*, 2009; *de Gouw et al.*, 2005; *Heald et al.*, 2005, 2006; *Johnson et al.*, 2006; *Kleinman et al.*, 2008; *Volkamer et al.*, 2006]. Such difficulties likely arise from complexity in the sources (including both primary combustion emissions, POA, and secondary production SOA), composition, and chemistry of OA. While traditionally SOA has been thought to consist of products from a few classes of compounds (terpenes and aromatics), recent studies have identified both additional precursors [*Kroll et al.*, 2005; *Lim and Ziemann*, 2009; *Robinson et al.*, 2007; *Volkamer et al.*, 2009] and additional formation pathways [*Carlton et al.*, 2007; *Kalberer et al.*, 2004]. Once formed in the atmosphere, the pool of OA remains dynamic, through both reversible partitioning and continued atmospheric oxidation. This additional processing ("aging") is generally not well-represented in models as it involves a number of physical and chemical processes that are typically not accessed in laboratory experiments. Furthermore, air mass mixing in the atmosphere implies a blending of OA from various sources. In this study, we identify compositional characteristics shared by atmospheric OA formed under a wide range of reaction conditions (different environments, precursors, volatilities, and photochemical ages) using a Van Krevelen diagram.

2. Van Krevelen Diagram

[3] The Van Krevelen diagram was developed to illustrate how elemental composition changes during coal formation [*Van Krevelen*, 1950]. The diagram cross plots the hydrogen to carbon atomic ratio (H:C) and the oxygen to carbon atomic ratio (O:C). It has seen recent use for the graphical interpretation of ultra-high resolution mass spectrometric data, in which the elemental ratios of individual compounds are plotted instead of those of the bulk material [*Kim et al.*, 2003]. This approach has recently been applied towards the mass spectrometric measurement of individual species within atmospheric OA [e.g., *Bateman et al.*, 2009], but to our knowledge has not been used for bulk aerosol measurements.

[4] Figure 1 shows a conceptual Van Krevelen diagram for organic material in the atmosphere, where the most oxidized species lie at the lower right. This space can be used to illustrate how reactions involving the addition of functional groups fall along straight lines. For example, the replacement of an aliphatic carbon ($-CH_{2-}$) with a carbonyl group ($-C(=O)-$) implies a loss of 2 hydrogens and a gain of 1 oxygen, and thus a slope of −2 in the Van Krevelen diagram. Conversely, the replacement of a hydrogen with an alcohol group ($-OH$) involves an increase in oxygen but no change in hydrogen, and therefore is a horizontal line in Van Krevelen space. An intermediate slope of −1 is produced by the simultaneous addition of both functional groups, forming a hydroxycarbonyl or carboxylic acid. Organic atmospheric functionalization reactions, including, but not limited to those shown here, generally involve changes not only to O:C but also to H:C. While increasing O:C is often considered an indicator of atmospheric oxidation [e.g., *DeCarlo et al.*, 2008], Figure 1 shows that a non-oxidative process such as hydration reactions can be misinterpreted based on this limited description.

[1]Department of Atmospheric Science, Colorado State University, Fort Collins, Colorado, USA.
[2]Department of Civil and Environmental Engineering, Massachusetts Institute of Technology, Cambridge, Massachusetts, USA.
[3]CIRES and Department of Chemistry and Biochemistry, University of Colorado, Boulder, Colorado, USA.
[4]CIRES and Department of Atmospheric and Oceanic Sciences, University of Colorado, Boulder, Colorado, USA.
[5]Now at Paul Scherrer Institute, Villigen, Switzerland.
[6]Now at ETH Zurich, Zurich, Switzerland.
[7]School of Engineering and Applied Sciences and Department of Earth and Planetary Sciences, Harvard University, Cambridge, Massachusetts, USA.
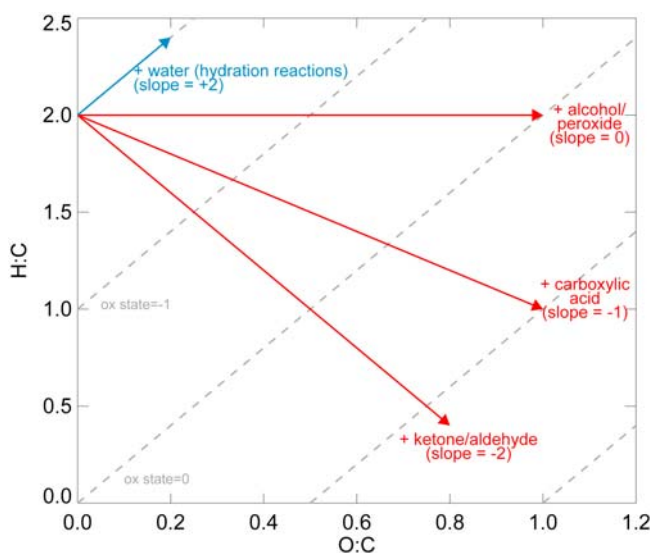[8]Instituto de Física, Universidade de São Paulo, Sao Paulo, Brazil.

Figure 1. Van Krevelen diagram illustrating how functionalization reactions of organic species affect H:C and O:C from an arbitrary starting point. Each arrow corresponds to the addition of a particular functional group to an aliphatic (unfunctionalized) carbon. Lines of constant carbon oxidation state are shown in grey.

Conversely, the oxidation of an alcohol to a carbonyl involves no change to O:C.

3. Application of the Van Krevelen Diagram to Atmospheric Aerosol

[5] Atmospheric OA consists of a multitude of compounds with a wide range of properties. Typically less than 20% of the mass of OA can be speciated [*Williams et al.*, 2007]. Estimation of bulk elemental ratios can provide insight into the composition of OA in the atmosphere. One recently used method utilizes data from the Aerodyne high resolution aerosol mass spectrometer (HR-AMS). The HR-AMS provides mass spectra of an ensemble of submicron OA particles in real time, with sufficiently high mass resolution that the chemical formulae of all important ions (especially below $m/z \leq 100$) can be unambiguously determined [*DeCarlo et al.*, 2006]. As demonstrated by *Aiken et al.* [2007, 2008], summation of the abundances of each element within each ion, and correction by an empirical factor to account for biases in ion fragmentation, allows for the determination of elemental ratios (O:C and H:C) of the OA. Results for individual organics are somewhat uncertain (with errors of ~30% for O:C and 10% for H:C [*Aiken et al.*, 2007]), but these uncertainties are likely to be substantially lower for the large ensemble of organics found in ambient aerosol, due to averaging of non-systematic errors. Elemental ratios estimated from AMS measurements from several laboratory and field measurements are explored here.

[6] Figure 2 shows a Van Krevelen diagram of the bulk composition of OA. Mean values from field experiments are shown as solid circles. These include the Study of Organic Aerosol at Riverside (SOAR-1) campaign in Riverside, California in summer 2005, the Amazonian Aerosol Characterization Experiment (AMAZE-08) in the central Amazon

Basin, during the wet season of 2008 [*Chen et al.*, 2009], and both the aircraft and T0 site during the Megacity Initiative: Local and Global Research Observations (MILAGRO) campaign in Mexico City in Spring 2006 [*Aiken et al.*, 2008; *DeCarlo et al.*, 2008]. Also shown is the elemental composition of the individual Positive Matrix Factorization factors during MILAGRO. These factors have been shown to represent freshly emitted OA (HOA, BBOA) and more oxidized OA (progressing from OOA2 to "aged" OOA1) [*Aiken et al.*, 2008]. Laboratory studies are shown with diamonds. These include a series of vehicle and biomass burning POA (diesel, gasoline, smoke from lodgepole pine and sage/rabbitbrush burning) from *Aiken et al.* [2008], laboratory-generated SOA from α-pinene ozonolysis at decreasing OA mass loadings (from left to right) [*Shilling et al.*, 2009] and the products of heterogeneous oxidation of squalane with increasing OH exposure (from left to right) [*Kroll et al.*, 2009]. Finally, the evolution of the elemental composition of OA for a series of thermo-denuder experiments (with temperature increasing left to right) is shown as open circles [*Huffman et al.*, 2009]. All these data line up in the Van Krevelen diagram along a line with a slope of ~−1.

[7] Figure 3 shows the Van Krevelen diagrams for the complete set of OA measurements from three field campaigns (SOAR-1, AMAZE-08, and MILAGRO) where measurements line up approximately with the −1 slope (slopes of −1.1, −1.1, 0.8 fitted with reduced-major axis approach) with Pearson correlation coefficients of −0.90, −0.64 and −0.62 respectively. The aerosols sampled at Riverside exhibit a limited range of composition, which likely reflects predominantly anthropogenic sources of OA, both primary and secondary, transported from the center of the Los Angeles basin. Aerosol loadings at the AMAZE-08 site, are substantially lower [*Chen et al.*, 2009] which may explain the higher degree of scatter on the elemental ratios. OA in this clean, forested environment exhibits a wide range of oxygen content, with more oxidized aerosol than observed at Riverside. This may be the result of differences in aerosol sources, level of aging, and/or aerosol loading. Given the more extensive sampling of source types and air mass ages possible aboard an aircraft compared to a single field site, the observations made aboard the C-130 during the MILAGRO campaign likely reflect the most diverse dataset here. These measurements are colored by a photochemical clock representing the conversion of nitrogen oxides to total reactive nitrogen. We find that the aerosol composition generally appears to move down this composition line in Van Krevelen space, as a function of photochemical age.

4. Discussion

[8] Figures 2 and 3 illustrate that OA occupies a remarkably narrow linear area in Van Krevelen space, indicating a tight coupling between particulate H:C and O:C. Thus OA has a characteristic bulk elemental composition, with a rough empirical formula of $CH_{2-x}O_x$ (x = 0−1). This holds true for a wide range of OA types - laboratory/ambient, biogenic/anthropogenic, urban/remote, and freshly emitted/aged. It should be emphasized that since Van Krevelen plots provide no information on molecular structure or carbon number, the molecular species in each case are almost certainly different, even if the average elemental compositions are the same. Moreover, all reported elemental ratios are bulk measure-
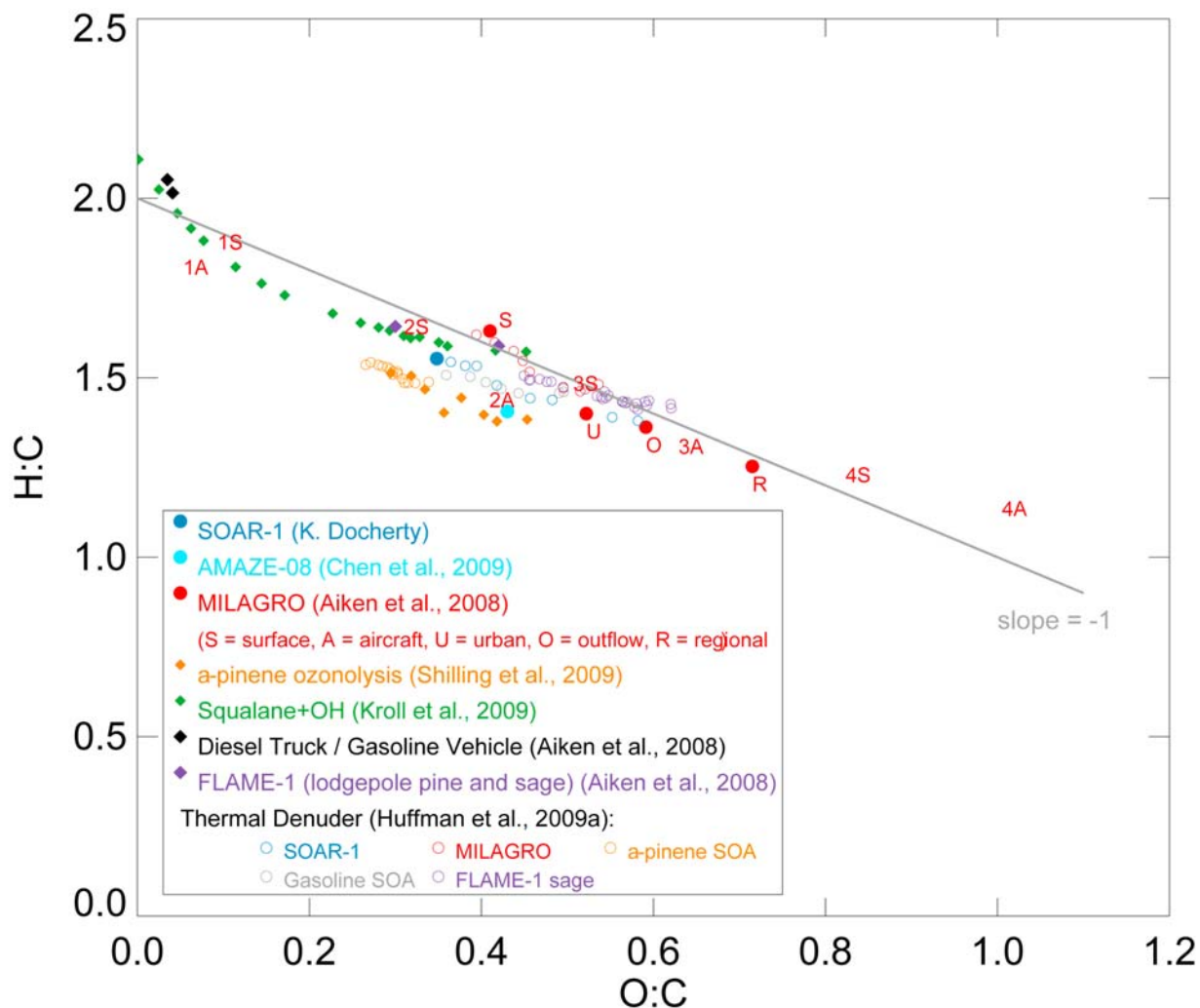
Figure 2. Van Krevelen diagram of elemental ratios estimated from HR-AMS measurements of organic aerosol. These include mean observations from field studies (solid circles), lab studies (diamonds), and thermal denuder experiments (open circles). Also shown are the positive matrix factorization components of the MILAGRO observations (1 = HOA, 2 = BBOA, 3 = OOA2, 4 = OOA1) [*Aiken et al.*, 2008]. Line with −1 slope is illustrative and originates at O:C = 0 and H:C = 2, corresponding to an arbitrarily long acyclic alkane.

ments, the averages of a very large number of different molecules, and individual species have a much wider range of H:C and O:C. Indeed, ultrahigh-resolution electrospray ionization mass spectrometry of SOA [e.g., *Bateman et al.*, 2009] results in Van Krevelen plots that are roughly centered on the fitted line, but with a good deal of spread in both the H:C and O:C dimensions. At the same time, the fact that aerosol sampled at different loadings [*Shilling et al.*, 2009] and temperatures [*Huffman et al.*, 2009] fall along the same line indicates that aerosol components of different volatilities do not deviate substantially from this general elemental composition trend, and that volatilization processes involve movement along this line.

[9] As oxidation involves movement towards the right (higher O:C) and the bottom (lower H:C) of the Van Krevelen diagram (Figure 1), the data in Figures 2 and 3 span a range of oxidation of the OA. The trajectory defined by the fitted line in the Van Krevelen diagram can represent some combination of physical mixing and aerosol aging (oxidation, volatilization, condensation). While these processes are inex-

tricable for field studies, the laboratory results [*Huffman et al.*, 2009; *Kroll et al.*, 2009; *Shilling et al.*, 2009] shown in Figure 2 strongly suggest that the fitted line defines an average elemental trajectory associated with aerosol aging. The slope of −1 indicates that for each oxygen atom added upon oxidation, a hydrogen atom is lost. This change is consistent with equal increases in carbonyl and alcohol moieties, such as carboxylic acid addition (Figure 1) as well as with the observed increase in the intensity of the *m/z* 44 ion (thought to be a marker of acid groups in AMS measurements [*Aiken et al.*, 2008]).

[10] Ambient measurements also scatter around the −1 slope in the Van Krevelen diagram. In particular, the MILAGRO measurements of OA at different photochemical ages suggest a trajectory towards more oxidized aerosol with time (Figure 3c), Physical mixing of fresh POA (O:C~0, H:C~2) with more oxygenated OA (O:C~0.5, H:C~1.5) can generate the observed −1 slope, but is likely to play a role only in close proximity to emission sources. This may contribute to the strong correlation observed at the Riverside site (Figure 3a).
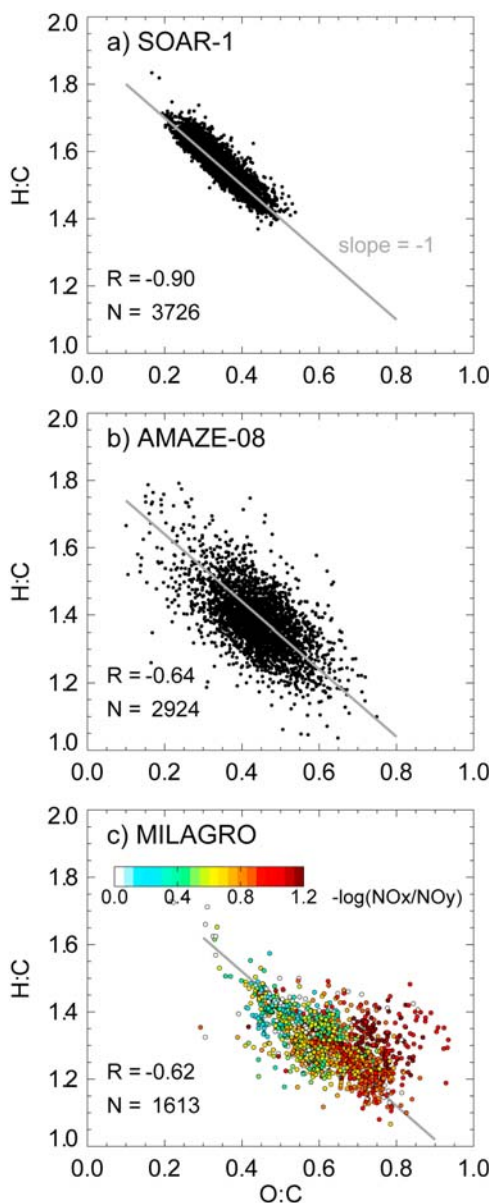
Figure 3. Van Krevelen diagrams of the elemental ratios of organic aerosol measured by AMS during (a) the SOAR-1 campaign at Riverside, CA (5 minute average); (b) the AMAZE-08 campaign in the Central Amazon Basin (5 minute average); (c) the MILAGRO C-130 aircraft campaign over Mexico City (1 minute average) colored by a photochemical clock, represented by the conversion of nitrogen oxides (NO_x) to total reactive nitrogen (NO_y). Lines with -1 slope are illustrative. Correlation coefficient (R) and number of observations (N) are shown. Low loadings increase the uncertainty in elemental analysis, thus observations with OA loadings less than 0.3 $\mu g/m^3$ are not shown.

[11] This general relationship related to the elemental composition of the aerosol can be used to assess the potential importance of individual species or processes. For example, given that isoprene tetrols (O:C = 0.8, H:C = 2.4) or glyoxal oligomers (which involves the addition of two water molecules, such that O:C = 1.25−2 and H:C = 1.5−3 for n = 1−4) lie substantially above the line in Figures 2 and 3, their presence would need to be balanced by compounds with low H:C and O:C, suggesting that they do not make up a major fraction of mass of the aerosol studied. Similarly, hydration/dehydration reactions sometimes associated with oligomerization reactions of particulate organics, involve movement in Van Krevelen space inconsistent with observations, suggesting they do not dominate the evolution of atmospheric aerosol.

[12] It should be noted that the slope or intercept of the best-fit line for some individual datasets is somewhat different than that shown in Figure 2. The line originates at O:C = 0 and H:C = 2, corresponding to an alkene or cycloalkane (or arbitrarily long acyclic alkane). However, some of the individual data sets shown, while exhibiting a slope of ~−1, have a somewhat lower y-intercept; examples include the two datasets of SOA from α-pinene ozonolysis [*Huffman et al.*, 2009; *Shilling et al.*, 2009] as well as the AMAZE-08 observations (from a site heavily influenced by isoprene chemistry). Such differences may result from the fact that the SOA precursors fall well below the fitted line (H:C$_{terpene}$ = 1.6). However, the y-intercepts (~1.8) are not quite as low, indicating that the formation of condensable products involved the addition of O with no loss (and possibly a gain) of H, in accordance with known mechanisms [*Calvert et al.*, 2000]. The same is also likely to hold true for SOA from other polyunsaturated species, such as aromatic hydrocarbons (e.g., H:C$_{toluene}$ = 1.14). Moreover, the interpretation of the aerosol composition as a pure H-C-O system does not account for nitrogen or sulfur containing moieties. These might influence measured O:C or H:C, and may in fact explain some of the scatter observed in the measurements made in urban/polluted areas (Figure 3).

[13] While the dominant compositional changes observed proceed along a ~−1 slope, this tight compositional relationship does not hold for all of the datasets. Much of the MILAGRO data (Figure 3c) follows the −1 slope but levels off at high oxidation levels (reducing the overall fitted slope to −0.8). The heterogeneous oxidation of squalane (green diamonds in Figure 2) shows a similar shallow slope at high O:C. This may suggest the greater tendency for alcohol addition, or the increased importance of C-C bond breaking (fragmentation) reactions, which lead to relatively small changes in H:C. For example, if a carboxylic acid group is added to the site of a C-C bond cleavage, as suggested by recent experimental work [*Kroll et al.*, 2009], the net effect would be to replace a −CH$_2$− group with a −COOH group, for a slope of only −1/2. The composition trend in squalane oxidation in fact appears never to follow the −1 slope. This may represent a contrast between a single-compound experiment versus a complex atmospheric system where the multiplicity of molecular structures and oxidation pathways average out variability. Further studies of multigenerational oxidative processing are necessary to better understand how the abundances of individual functional groups change upon aging or volatilization in the atmosphere.

5. Conclusions

[14] The development of accurate models of OA processing in the atmosphere has been stymied by both a paucity of laboratory constraints on these processes, and the computational cost implicit in a detailed chemical description of these reactions. Atmospheric OA is shown here to have a narrow

range of bulk elemental composition, despite the large diversity of constituent molecules. H:C and O:C of a wide range of aerosol types are related linearly, with a ~ -1 slope in Van Krevelen space. Volatilization and oxidative aging, two key physical and chemical processes that OA is subject to after emission or formation, both involve movement along this line, resulting in a more oxidized aerosol. Mixing of fresh and aged air masses may also produce a similar OA trajectory. These results suggest that the chemical evolution of OA in the atmosphere may be simply represented in models. Development of a generalized scheme requires further investigation of the time scales for this aging in different environments. A complete description of OA processing must link these compositional changes with key physical properties (e.g., volatility, hygroscopicity, light absorption) of the aerosol.

References

Aiken, A. C., et al. (2007), Elemental analysis of organic species with electron ionization high-resolution mass spectrometry, *Anal. Chem.*, *79*(21), 8350–8358, doi:10.1021/ac071150w.

Aiken, A. C., et al. (2008), O/C and OM/OC ratios of primary, secondary, and ambient organic aerosols with high-resolution time-of-flight aerosol mass spectrometry, *Environ. Sci. Technol.*, *42*(12), 4478–4485, doi:10.1021/es703009q.

Bateman, A. P., et al. (2009), Time-resolved molecular characterization of limonene/ozone aerosol using high-resolution electrospray ionization mass spectrometry, *Phys. Chem. Chem. Phys.*, *11*(36), 7931–7942, doi:10.1039/b905288g.

Calvert, J. G., et al. (2000), *The Mechanisms of Atmospheric Oxidation of the Alkenes*, Oxford Univ. Press, Oxford, U. K.

Capes, G., et al. (2009), Secondary organic aerosol from biogenic VOCs over West Africa during AMMA, *Atmos. Chem. Phys.*, *9*(12), 3841–3850.

Carlton, A. G., et al. (2007), Atmospheric oxalic acid and SOA production from glyoxal: Results of aqueous photooxidation experiments, *Atmos. Environ.*, *41*(35), 7588–7602, doi:10.1016/j.atmosenv.2007.05.035.

Chen, Q., et al. (2009), Mass spectral characterization of submicron biogenic organic particles in the Amazon Basin, *Geophys. Res. Lett.*, *36*, L20806, doi:10.1029/2009GL039880.

de Gouw, J. A., et al. (2005), Budget of organic carbon in a polluted atmosphere: Results from the New England Air Quality Study in 2002, *J. Geophys. Res.*, *110*, D16305, doi:10.1029/2004JD005623.

DeCarlo, P. F., et al. (2006), Field-deployable, high-resolution, time-of-flight aerosol mass spectrometer, *Anal. Chem.*, *78*(24), 8281–8289, doi:10.1021/ac061249n.

DeCarlo, P. F., et al. (2008), Fast airborne aerosol size and chemistry measurements above Mexico City and central Mexico during the MILAGRO campaign, *Atmos. Chem. Phys.*, *8*(14), 4027–4048.

Heald, C. L., D. J. Jacob, R. J. Park, L. M. Russell, B. J. Huebert, J. H. Seinfeld, H. Liao, and R. J. Weber (2005), A large organic aerosol source in the free troposphere missing from current models, *Geophys. Res. Lett.*, *32*, L18809, doi:10.1029/2005GL023831.

Heald, C. L., et al. (2006), Concentrations and sources of organic carbon aerosols in the free troposphere over North America, *J. Geophys. Res.*, *111*, D23S47, doi:10.1029/2006JD007705.

Huffman, J. A., et al. (2009), Chemically-resolved volatility measurements of organic aerosol from different sources, *Environ. Sci. Technol.*, *43*(14), 5351–5357, doi:10.1021/es803539d.

Johnson, D., et al. (2006), Simulating regional scale secondary organic aerosol formation during the TORCH 2003 campaign in the southern UK, *Atmos. Chem. Phys.*, *6*, 403–418.

Kalberer, M., et al. (2004), Identification of polymers as major components of atmospheric organic aerosols, *Science*, *303*(5664), 1659–1662, doi:10.1126/science.1092185.

Kim, S., et al. (2003), Graphical method for analysis of ultrahigh-resolution broadband mass spectra of natural organic matter, the Van Krevelen diagram, *Anal. Chem.*, *75*(20), 5336–5344, doi:10.1021/ac034415p.

Kleinman, L. I., et al. (2008), The time evolution of aerosol composition over the Mexico City plateau, *Atmos. Chem. Phys.*, *8*(6), 1559–1575.

Kroll, J. H., N. L. Ng, S. M. Murphy, R. C. Flagan, and J. H. Seinfeld (2005), Secondary organic aerosol formation from isoprene photooxidation under high-NO_x conditions, *Geophys. Res. Lett.*, *32*, L18808, doi:10.1029/2005GL023637.

Kroll, J. H., et al. (2009), Measurement of fragmentation and functionalization pathways in the heterogeneous oxidation of oxidized organic aerosol, *Phys. Chem. Chem. Phys.*, *11*, 8005–8014, doi:10.1039/b905289e.

Lim, Y. B., and P. J. Ziemann (2009), Chemistry of secondary organic aerosol formation from OH radical-initiated reactions of linear, branched, and cyclic alkanes in the presence of NO_x, *Aerosol Sci. Technol.*, *43*(6), 604–619, doi:10.1080/02786820902802567.

Robinson, A. L., et al. (2007), Rethinking organic aerosols: Semivolatile emissions and photochemical aging, *Science*, *315*(5816), 1259–1262, doi:10.1126/science.1133061.

Shilling, J. E., et al. (2009), Loading-dependent elemental composition of alpha-pinene SOA particles, *Atmos. Chem. Phys.*, *9*(3), 771–782.

Van Krevelen, D. W. (1950), Graphical-statistical method for the study of structure and reaction processes of coal, *Fuel*, *24*, 269–284.

Volkamer, R., J. L. Jimenez, F. San Martini, K. Dzepina, Q. Zhang, D. Salcedo, L. T. Molina, D. R. Worsnop, and M. J. Molina (2006), Secondary organic aerosol formation from anthropogenic air pollution: Rapid and higher than expected, *Geophys. Res. Lett.*, *33*, L17811, doi:10.1029/2006GL026899.

Volkamer, R., et al. (2009), Secondary organic aerosol formation from acetylene (C_2H_2): Seed effect on SOA yields due to organic photochemistry in the aerosol aqueous phase, *Atmos. Chem. Phys.*, *9*(6), 1907–1928.

Williams, B. J., A. H. Goldstein, D. B. Millet, R. Holzinger, N. M. Kreisberg, S. V. Hering, A. B. White, D. R. Worsnop, J. D. Allan, and J. L. Jimenez (2007), Chemical speciation of organic aerosol during the International Consortium for Atmospheric Research on Transport and Transformation 2004: Results from in situ measurements, *J. Geophys. Res.*, *112*, D10S26, doi:10.1029/2006JD007601.

Zhang, Q., et al. (2007), Ubiquity and dominance of oxygenated species in organic aerosols in anthropogenically-influenced Northern Hemisphere midlatitudes, *Geophys. Res. Lett.*, *34*, L13801, doi:10.1029/2007GL029979.

A. C. Aiken, ETH Zurich, Rämistrasse 101, CH-8092 Zurich, Switzerland.

P. Artaxo, Instituto de Fisíca, Universidade de São Paulo, Caixa Postal 66318, 05315-970 Sao Paulo, Brazil.

Q. Chen and S. T. Martin, School of Engineering and Applied Sciences, Harvard University, 29 Oxford St., Cambridge, MA 02138, USA.

P. F. DeCarlo, Paul Scherrer Institute, CH-5232 Villigen PSI, Switzerland.

K. S. Docherty, D. K. Farmer, and J. L. Jimenez, CIRES, University of Colorado, UCB 216, Boulder, CO 80309, USA.

C. L. Heald, Department of Atmospheric Science, Colorado State University, 1371 Campus Delivery, Fort Collins, CO 80525, USA. (heald@atmos.colosate.edu)

J. H. Kroll, Department of Civil and Environmental Engineering, Massachusetts Institute of Technology, 77 Massachusetts Ave., Room 1-290, Cambridge, MA 02139-4307, USA.